Documenta Ophthalmologica **104:** 249–276, 2002.

An Expanded Nystagmus Acuity Function: Intra- and Intersubject Prediction of Best-Corrected Visual Acuity

L.F. DELL'OSSO[1,2,3] and J.B. JACOBS[1,3]
From the Ocular Motor Neurophysiology Laboratory[1], Veterans Affairs Medical Center; and the Departments of Neurology[2] and Biomedical Engineering[3], Case Western Reserve University, Cleveland, OH, USA

Accepted 2 August 2001

Abstract. The Nystagmus Acuity Function (NAF) provides an objective measurement of the foveation characteristics of nystagmus waveforms and an assessment of *potential* visual acuity for subjects with congenital (CN) or latent/manifest latent (LMLN) nystagmus. It is based on the subjects' ability to maintain fixation within a physiologically based 'foveation window' of $\pm 0.5°$ and $\pm 4.0°/s$. However, some subjects are incapable of controlling fixation well enough to remain within this window with duration sufficient for good foveation. To obtain a measure of the CN waveforms of these individuals, we are proposing an eXpanded Nystagmus Acuity Function (NAFX) that relaxes either the position limit, the velocity limit, or both. Data used in this study comes from 11 human subjects with CN (10 idiopathic and 1 with achiasma) and a Belgian sheepdog with achiasma. Visual acuity was tested with a standard Snellen chart and eye movements recorded with infrared oculography or scleral search coil. For the NAFX to be useful, it must not only be applicable for subjects who cannot maintain fixation within the standard limits of the NAF, but also must yield results *equivalent* to those obtained with the NAF when testing subjects who are capable of maintaining good fixation control. For the latter subjects, the amount of time when position and velocity fell within the expanded limits was measured, the standard deviations of the position and velocity during these times were calculated, and a τ-surface for the exponential function was generated to guarantee the equivalence between the NAF and the NAFX. We developed an automated NAFX equivalent to the original NAF. We demonstrated that equivalence in 10 subjects and the use of the NAFX on two additional (1 human and 1 canine) subjects who were incapable of maintaining fixation within the standard position and velocity limits. We demonstrated the effects of surgery and related the results to visual acuity. We found the results to be comparable to those seen when applying the NAF to subjects who had good fixation control. The NAFX can be determined for CN and LMLN subjects with poor control of fixation by extending the standard NAF position and/or velocity limits for foveation. The resulting function can be used along with the longest foveation domain (derived from the NAFX to measure breadth of a high-NAFX region) to identify the gaze or convergence angles with the best waveform and to predict the best-possible visual acuity that could be achieved with the reduction of their nystagmus.

Key words: congenital nystagmus, eye movements, eye muscle surgery, visual acuity, waveform function

Abbreviations: CN – congenital nystagmus; IR – infrared; LED – light-emitting diode; LMLN – latent/manifest latent nystagmus; NAF – nystagmus acuity function; NAFX – expanded nystagmus acuity function

Introduction

The visual acuity of an individual with nystagmus, whether congenital nystagmus (CN), latent/manifest latent nystagmus (LMLN), or another type of nystagmus, is dependent on both the afferent visual system and certain characteristics of the nystagmus waveform. In the absence of an uncorrected, afferent, acuity-limiting deficit, these waveform characteristics alone determine the best-corrected visual acuity. In the past, due to the absence of viable alternatives, CN waveforms were judged by characteristics that were only indirectly related to visual acuity. They included: peak-to-peak amplitude (or the related characteristics, intensity or slow-phase velocity) [1–5]; intervals of slow-phase velocity below an arbitrarily defined threshold [6,7]; or intervals of eye position near the center of the fovea [8]. The latter two have been incorrectly equated to 'foveation' periods, despite the lack of target foveation possible in the former and high retinal slip velocity possible in the latter definition. Although each of these putative measures of acuity seems reasonable, they all depend on presumptions that are usually violated by many CN waveforms. Some are better than others for intrasubject comparisons if the waveform is consistent. However, for most subjects (who have more than one waveform) and for intersubject comparisons, none of these measures is adequate.

Figure 1 illustrates pairs of CN waveforms that demonstrate how application of the above *measures* of waveform characteristics used to assess the effects of therapy and to predict visual acuity, may be expected to *fail* to do the latter. In the top comparison, the waveform on the left has both a larger peak-to-peak amplitude (|CN|) and a higher slow-phase velocity. However, because it also has longer foveation periods, it should allow higher acuity than the waveform on the right. In such cases, neither amplitude (or intensity) nor slow-phase velocity would accurately predict visual acuity. In the second comparison from the top, the waveform on the right has longer 'foveation' periods (here, defined simply as intervals of low eye velocity) but, due to the large position *jitter* of the waveform, it would allow lower acuity than the waveform on the left that exhibits accurate foveation. In the next comparison, the 'foveation' periods are equal in both waveforms but again the large position jitter in the right waveform should result in a lower acuity than that allowed with the left waveform. Also, the use of an eye-velocity

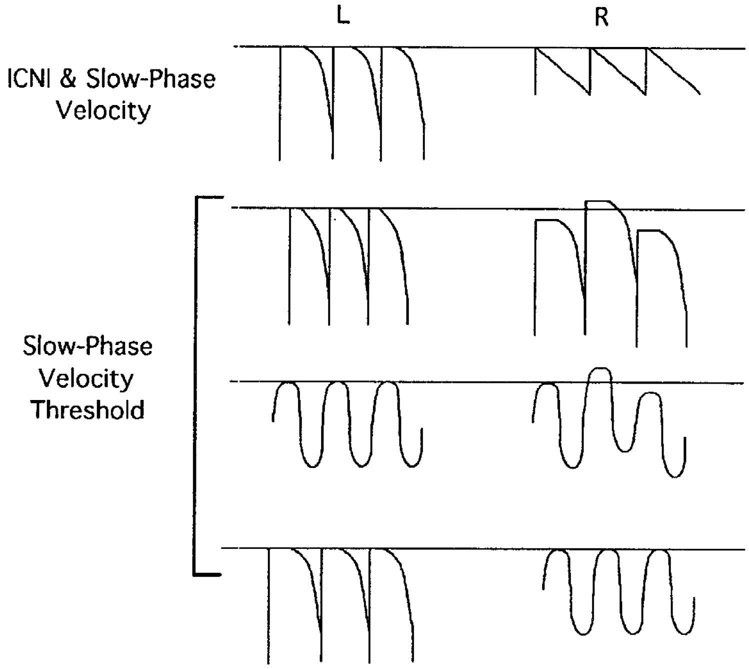

Figure 1. Illustrations of variations in CN waveforms and their effects on visual acuity. Comparisons between the left (L) and right (R) pairs of waveforms reveal the problems inherent in using some of the measures (listed on the left) commonly claimed to be related to visual acuity. In the first three (from the top) comparisons, the waveforms shown under the L result in higher acuity than those shown under the R; the two waveforms in the bottom comparison yield equal acuities. Horizontal lines indicate target position for each case.

threshold to predict acuity fails for pendular waveforms because, except for very low-amplitude nystagmus, such 'foveation' periods at one extreme of the oscillation do not contribute to acuity significantly, since the target image is far from the fovea. Finally, the bottom comparison shows two waveforms that should allow equal acuities despite the fact that the one on the right has twice as many data points whose velocity falls below a predetermined threshold. Thus, for these common pendular or jerk CN waveforms, one could not expect to accurately predict visual acuity by considering *only* those intervals when either the eye position falls on the target or the eye velocity falls below an arbitrary threshold. Good visual acuity requires the *simultaneous satisfaction* of two criteria: repeated foveation of the target and low retinal slip velocity for extended time intervals – that is the definition of *well-developed foveation* [8].

It has long been recognized that a better, objective measure, based on specific waveform characteristics (quality) directly related to length of target foveation, was needed to identify the regions of best possible acuity, assess and compare the results of therapy, and predict the upper limits of acuity possible, based on waveform improvement alone [2, 8–12]. Because of these considerations, a Nystagmus Acuity Function (NAF) was developed to provide an objective measure of the quality of a nystagmus waveform, to predict best-corrected visual acuity in CN and LMLN patients under benign conditions, and used to assess the effects of afferent stimulation on CN [9]. It is important that such a function minimizes the idiosyncratic effects of anxiety and afferent deficits or they might confound intra- and inter-subject determinations and comparisons of regions of best acuity or therapeutic effects.

The NAF is a function that predicts the best-corrected visual acuity possible in subjects with nystagmus, based on objective measurement of their waveform characteristics during fixation of a small light-emitting diode. It combines the foveation time per cycle and the standard deviations of both eye position and velocity during target foveation into a function that is linearly proportional to best-possible visual acuity. Because of idiosyncratic variations in CN waveforms and their foveation periods, satisfaction of *both* position and velocity criteria are necessary to calculate NAF values that can be reliably compared across subjects. The NAF uses a 'foveation window' of $\pm 0.5°$ by $\pm 4°/\mathrm{s}$ as the basis for calculating foveation. The dimensions of this window were derived from the anatomy of the foveal extent and normal data on the effects of retinal slip velocity on acuity. The nystagmus acuity function is defined by:

$$NAF = (1 - \sigma_{pv})[1 - \epsilon^{-t_f/\tau}]$$

where the pooled estimator

$$\sigma_{pv} = \sqrt{(SD_p^2 + SD_v'^2)/2},\ SD_v' = 0.125(SD_v)$$

t_f is the foveation-period duration, and the time constant, τ=33.3 msec [13, 14]. This value of τ was derived for use in the NAF using data from acuity studies of normals. Because of the pronounced effects of psychological state on CN waveforms (and, therefore, on acuity) [2,10,15] all measurements used to calculate the NAF are carried out in a dimly lit room with only light-emitting diodes as targets; that is, the task is easy and non-threatening. In this way, data can be accumulated that diminishes the variable effects of anxiety on CN and thereby allows for more accurate intra- and intersubject comparisons. The NAF values of nine subjects with CN, no afferent deficits, and no clinical changes in their CN during acuity measurement, were plotted against their measured visual acuities along with the best linear fit. The resulting line was used to predict the best possible acuity based on the NAF value. The presumption in those cases was that the waveforms during acuity testing were not significantly different than those recorded for NAF calculation; we recognize that this is often not the case. Although a given individual may not achieve the best-corrected visual acuity predicted by the NAF because of the anxiety of taking a visual acuity test, under more benign real-world conditions the actual acuity should approach the NAF predictions.

It is important to remember that the quality of the CN waveform used to calculate the NAF was, in part, influenced by the benign conditions and easy visual task we employ during recordings. These conditions and mental set can change radically during a visual acuity test. Thus, for most subjects we *expect* that plotting their NAF-acuity data pairs on this type of graph will result in data points that fall *below* the NAF vs. best-possible acuity line. The two measures were made at different times under different conditions. The exact amount by which these points fall below the line depends on factors not measured during the determination of either the NAF or acuity. These include the effects of anxiety on the CN waveform and the decrement in acuity due to associated afferent deficits, both difficult to quantify.

Since its development, we have used the NAF to evaluate both CN and LMLN subjects [9, 16]. For individuals, we have used it to identify gaze-angle and convergence regions of best acuity or the CN waveforms most conducive to better acuity. We also used it to compare waveform improvements and best-corrected visual acuity predictions pre- and post-therapy. Additionally, if the actual measured visual acuity is much worse than the best possible value predicted by the NAF, it is probable that an afferent deficit is the main reason, not the CN. The NAF is uniquely suited to evaluate the relationship between waveforms and acuity or therapies across subjects.

Unfortunately, there are a substantial number of individuals with nystagmus who cannot maintain, on a beat-to-beat basis, foveation within this stringent window (i.e. they do not have well-developed foveation). Instead, they exhibit either jitter of foveation position greater than $\pm 0.5°$ or of foveation velocity greater than $\pm 4°/s$, or both. A method of evaluating the CN waveforms and predicting the best-corrected visual acuity of these individuals for different therapies was also needed, whether the cause of the jitter was due solely to the ocular motor instability or was exacerbated by an afferent deficit. We developed an eXpanded Nystagmus Acuity Function, the NAFX, to assess the upper limits of the acuities of individuals with poor foveation capabilities [17]. Neither the NAFX nor the NAF, which it includes, are dependent on the methodology of data collection (e.g. infrared, video, or magnetic search coil), the type of nystagmus (CN, LMLN, etc.), or the particular nystagmus waveform.

To achieve this goal in a user-friendly method, we derived an algorithm that automatically determines the number of foveation periods present in an interval of eye movement data (usually 2–5 s). This had previously been done for the NAF by visual inspection of the records and required extensive experience in evaluation of nystagmus data. We next used data from a subject with CN and well-developed foveation to derive an average τ-surface for all combinations of position and velocity boundaries of the expanded foveation windows to be used in calculating the NAFX. That is, a surface of possible values for τ, each for a particular combination of position and velocity values, that result in the same value of the NAFX. The average τ-surface was calculated to force the values given by the NAFX for all possible window sizes to be equal to that of the NAF, thereby preserving its relationship to best-possible acuity. This requirement is dictated by the fact that the actual visual acuity of an individual remains unchanged despite the size of the foveation window used to calculate the NAFX and, therefore, so must the predicted upper limit of acuity. NAFX values were plotted against measured visual acuity for nine CN subjects whose foveation was well-developed. Finally, we applied the NAFX to evaluate the waveforms and to predict best-corrected visual acuity from the data of individuals with CN and either stress-diminished or poorly developed foveation.

In this paper, we present the theoretical foundations of the NAFX, the methods employed in its implementation, a demonstration of its equivalence to the original NAF in nine subjects, and examples of its use in the analysis of the CN of three additional subjects, two human and one canine. To demonstrate the breadth of the NAFX's utility, we chose one human subject (S1) with typical idiopathic CN and no sensory deficits, and at the other extreme, a subject (S2) with achiasma; the canine (S3), also had achiasma. Achiasma is a structural defect (the absence of an optic chiasm) that results in deficits in lateral geniculate and cortical mapping of visual inputs. We used the NAFX to identify regions where higher acuity might be expected for S1 and S2, and to assess the effects of a new surgery, tenotomy, on the CN waveform of S3.

Methods

Recording

The data used to demonstrate the NAF (9 human subjects) and the NAFX (2 human and one canine subjects) were recorded in several laboratories using both scleral search coil and infrared (IR) reflection techniques. Horizontal and vertical rotations of both eyes were recorded in the Ocular Motor Neurophysiology Lab using the scleral search coil method with 6-foot field coils (CNC Engineering, Seattle, WA). The coil system bandwidth was 0–150 Hz, linear range of greater than ±20° and sensitivity of 0.1° in both planes.

The subject's stabilized head remained within the 30-cm cube of the magnetic field where the translation artifact was less than 0.03°/cm. Data were filtered (bandwidth 0–90 Hz) and digitized at 200 Hz with 16-bit resolution using a DT2801/5716A (Data Translation, Marlboro, MA) board. Scleral-coil (Skalar, Delft, the Netherlands) gain was calibrated using a protractor device capable of rotations in each plane. Although calibrated, coil data was adjusted for bias during analysis. The mean foveation position of each eye was set to 0° to align it to the target position during fixation in primary position. This is routinely done for most other types of eye-movement recording methods and although it does not guarantee that the 0°-eye position coincides with a target image on the center of the fovea, it does place 0° at the subject's chosen point of fixation. Except for rare cases of extrafoveal fixation or certain types of foveal aplasia, it is reasonable to equate 0° with the foveal center, especially when the subject has good vision. Horizontal eye movement recordings were also made using infrared reflection. In the horizontal plane, the system is linear to ±20° and monotonic to ±25–30° with a sensitivity of 0.25°. Further details may be found elsewhere [18]. Some horizontal eye movement recordings were made using IR reflection (Applied Scientific Laboratories, Waltham, MA). The IR signal from each eye was calibrated with the other eye behind cover to obtain accurate position information and document small tropias and phorias hidden by the nystagmus. Eye positions and velocities (obtained by analog differentiation of the position channels) were displayed on a strip chart recording system (Beckman Type R612 Dynograph, Fullerton, CA). The total system bandwidth (position and velocity) was 0–100 Hz. IR data were digitized at 200 Hz with 12-bit resolution using a DT2801 (Data Translation, Marlboro, MA) board. Other data had been recorded by means of a phase-detecting revolving magnetic field technique in the Laboratory of R.M. Steinman. The sensor coils consisted of 9 turns of fine copper wire imbedded in an annulus of silicone rubber molded to adhere to the eye by suction. The signals were digitized at 488 Hz with a resolution of 16 bits. The system's sensitivity was less than one minute of arc, with linearity of one part in 14 014 and drift of 0.2–0.3 minarc/h. Noise was less than two minarc and eye position was stored to the nearest minarc. Further details of this system can be found elsewhere [19]. Finally, some of the data were recorded using a scleral search coil in the laboratory of H. Collewijn.

Protocol

During both search coil and IR recordings, subjects were seated in a chair with headrest and either a bite board or a chin stabilizer, far enough from the red light-emitting diodes (LEDs) (>5 feet) to prevent convergence effects except when testing fixation of near targets. During IR recording, subjects were seated at the center of a 5-ft radius arc containing LED targets. At this distance the LED subtended less than 0.1° of visual angle. During search-coil recording, the subject was seated 5 ft in front of a translucent screen upon which the targets were projected. During both, the head was stabilized in primary position and the subject was instructed to move only the eyes to view each target as it was turned on.

Written consent was obtained from subjects before the testing. All test procedures were carefully explained to the subject before the experiment began, and were reinforced with verbal commands during the trials. The room light could be adjusted from dim down to blackout to minimize extraneous visual stimuli. An experiment consisted of from one to 10 trials, each lasting under a minute with time allowed between trials for the subject to rest. Trials were kept this short to guard against boredom because CN intensity is known to decrease with inattention. This research, involving human subjects, followed the Declaration of Helsinki and informed consent was obtained after the nature and possible consequences of the study were explained. The research was approved by an institutional human experimentation committee.

Analysis

Data analysis (and filtering, if required), statistical computation of means and standard deviations, and graphical presentation were performed using the MATLAB (The MathWorks, Natick MA) software for scientific computing. We first developed an algorithm that identified all points that simultaneously satisfied the foveation window position and velocity criteria chosen and then made extrapolations to determine the number of foveation periods present in the data. The algorithm first identified all points that satisfied both the position and velocity criteria. Clusters of points were then grouped into foveation periods if they were longer than a predetermined duration (here, 7 ms). The number of successive sample points required varied with sampling rate to ensure that the duration criterion was met. Next, groups could be joined together if they were separated by less than 35 ms. These values come from studies based on tachistoscopic presentations. These rules insured that isolated points were not included, and foveation periods interrupted by just a few dropped points would not be counted more than once. The resulting software was then tested on a variety of CN data, including both jerk and pendular waveform variations, and was found to yield results equivalent to those obtained by expert analysis. The algorithm's performance was tested against and tuned to match, the manual, visual identification method used for the NAF in previous studies.

Using data sets from a typical, idiopathic CN subject with well-developed foveation (who did not require an expanded foveation window), we established a τ-surface for each data set for all expected combinations of expanded position and velocity boundaries; all NAFX values were forced to be equal to the NAF value. To calculate a τ-surface, we started with a segment of eye movement data from a CN subject known to have good foveation, i.e. capable of maintaining fixation in the original foveation window of 0.5° by 4.0°/s. The software then methodically expanded the position (0.5 – 6°) and velocity (4 – 10°/s) limits one at a time and searched, using an adaptive algorithm, for a new τ that gave the same result as the original NAF had for the initial foveation window. This yielded a surface of τ's, each one corresponding to a specific combination of position and velocity within the expanded limits. Several of these τ-surfaces, each from a different data set, were then averaged to yield the 'average τ-surface' that could be used for all data sets while satisfying the criterion that the resulting NAFX could not deviate from the NAF by more than 10%; this gave us an error-surface for that subject.

We then applied the NAFX, using the average τ-surface, to CN subjects with poor foveation who did require expanded foveation windows. The use of an average τ-surface, derived from the data of one subject with well-developed foveation, for all subjects regardless of their foveation abilities, is an extension of the use of a single τ to calculate the NAF for all subjects.

Theory behind the NAF(X)

The NAF, and later the NAFX, originated from the Nystagmus Foveation Function (NFF) [8] which incorporated the time-intervals of foveation periods and their position and velocity standard deviations into a measure of the *quality* of a CN waveform (i.e. how likely it was to allow good acuity). When calculated by hand, each cycle was assumed to have one foveation period and the number of cycles in the interval of interest was included in the calculation. Later, when the NAF(X) was automated, only 'true' foveation periods (i.e. those that satisfied the foveation-window criteria) were used in the calculation. For waveforms that exhibited well-developed foveation, this changed nothing. However, for poor foveation due to excessive jitter or high velocities, many cycles were deemed to have no foveation periods and the resulting NAF(X) reflected only those few foveation periods detected. This yielded very poor NAF(X) values that were not likely to be well correlated with acuity. To correct this problem, a measure of the total number of *potential* foveation periods (or cycles) needed to be reintroduced. This was most easily accomplished by applying the NAF(X) as described below.

Calculating the NAF(X)

To calculate NAF(X), it may occasionally be necessary to filter the position data (a digital fourth-order Butterworth low-pass with a 15 – 25 Hz cutoff and no phase distortion) and adjust the offset in the interval under consideration to center the nystagmus foveation periods on 0°. If the data are noise-free, prefiltering is unnecessary. There is an old computer adage that is appropriate here, 'garbage in, garbage out'. No matter how sophisticated an algorithm, poor input data will result in inaccurate, unreliable output data. We have developed this program using clean and accurate data from coil and IR systems in our laboratory and coil systems in the laboratories of R. M. Steinman and H. Collewijn. Because it is necessary to differentiate position data to obtain velocity data, noisy data from any source (especially, EOG) will not allow the accuracy required to predict acuity. Also, the interval used to calculate the NAF(X) must be one during which the subject was constantly fixating the LED target. It cannot contain blinks (or other artifacts) nor periods of inattention. In order to approximate complete cycles, the interval should begin and end at or before a foveating saccade. After differentiating the data to obtain velocity data, the NAF (default) function is called with its 'showpv' mode to display the number of true foveation periods. If the default NAF detects and displays a number of foveation periods greater than or equal to the number of CN cycles in the interval, the NAF function is applied in its 'naf' mode, using the actual number of cycles in which foveation periods were detected (including extras that were in the same CN cycle). However, if we observe that the output of the 'showpv' algorithm shows any cycles with no foveation period detected, the position limit of the foveation window is expanded just large enough to encompass all possible foveation periods in the interval to be used (i.e. presuming at least one foveation period per cycle). After rerunning 'showpv', if there are still cycles with undetected foveation periods, the velocity limit of the foveation window is then expanded to the lowest value that allows 'showpv' to detect one foveation period per CN cycle or, to the lowest value that maximizes the number of cycles in which foveation periods are detected. Thus, we progressively loosened the criteria for a foveation period until all (or, all possible) foveation periods in the data interval were detected. Finally, the 'nafx' mode is used with the position and velocity values chosen for the foveation window and the number of foveation periods detected by 'showpv'. Here, that number is set equal to the number of cycles in which foveation periods were detected by the algorithm (including extras, as above) plus the number of CN cycles for which no foveation periods were detected (if any). For most subjects, especially those with well-developed foveation, the value displayed by 'showpv' will be the correct one required for the NAFX calculation; if not, the display allows for easy identification of missed cycles. In either case, the software will display the NAF or NAFX, the average foveation time, the value of τ, and other data. An example of the command lines and program outputs is shown in the Appendix.

When attempting to predict the highest possible acuity of a nystagmus patient under a given condition (e.g. in primary position), the interval of data chosen should be the one with the highest NAFX calculated under that condition. To use the NAFX for determining the gaze or convergence angle of best possible acuity in a patient, one can either set the foveation window large enough for the poorest waveform and use that window for calculations at all other gaze/convergence angles or set the smallest window for the waveform at each angle; we have used both methods with success.

Results

In this section, we present the results of the application of the 'showpv' algorithm to determine foveation periods in a data set, and the results of algorithms that generate representative and average τ-surfaces for a subject with hereditary CN and well-developed foveation. We then apply the NAFX to an achiasmatic subject without well-developed foveation while fixating a distant target but with well-developed foveation at near. We also use the NAFX to predict the convergence or gaze angle at which the best acuity should occur. Finally, we use the NAFX to assess the results of the tenotomy procedure on the CN waveform of an achiasmatic canine.

Automated determination of foveation periods

The ability of a computer algorithm to detect all points in a segment of eye-movement data that simultaneously satisfy the NAF's foveation criteria ('showpv') is demonstrated in Figure 2A for S1, who had well-developed foveation. Except for the CN, S1 had a normal visual system with normal binocularity and no strabismus. All velocity (top) and position (middle) data points in this 5-s interval of distance fixation that fell within the defined foveation window are shown as thickened points superimposed on the CN pseudopendular with foveating saccades waveform. Note the presence of both single outliers and small, unthickened intervals lying between thickened sections of data. Figure 2A (bottom) demonstrates results of the application of a heuristic filter to the data; now only the 14 foveation periods satisfying the foveation-window criteria defined in the filter are shown thickened. Thus, all satisfactory foveation periods were automatically selected by the computer algorithm. Additionally, foveation-period duration data, see Figure 2B (top), and average position data, see Figure 2B (bottom), are depicted in the form

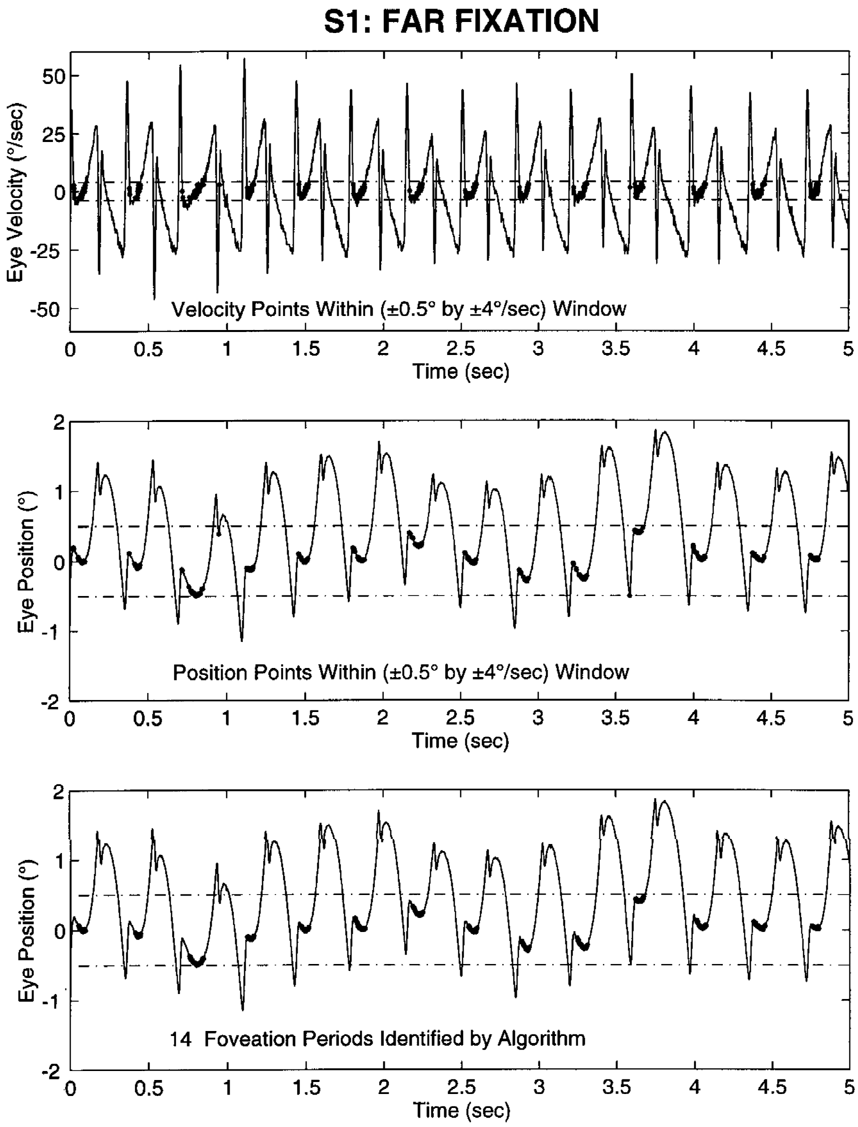

Figure 2a. (A) Example of the output of the NAFX 'showpv' algorithm that selects all points satisfying the desired velocity (top) and position (middle) foveation-window criteria and of the heuristic filter that selects the foveation periods (bottom). The selected foveation-period data from S1's far fixation are shown thickened.

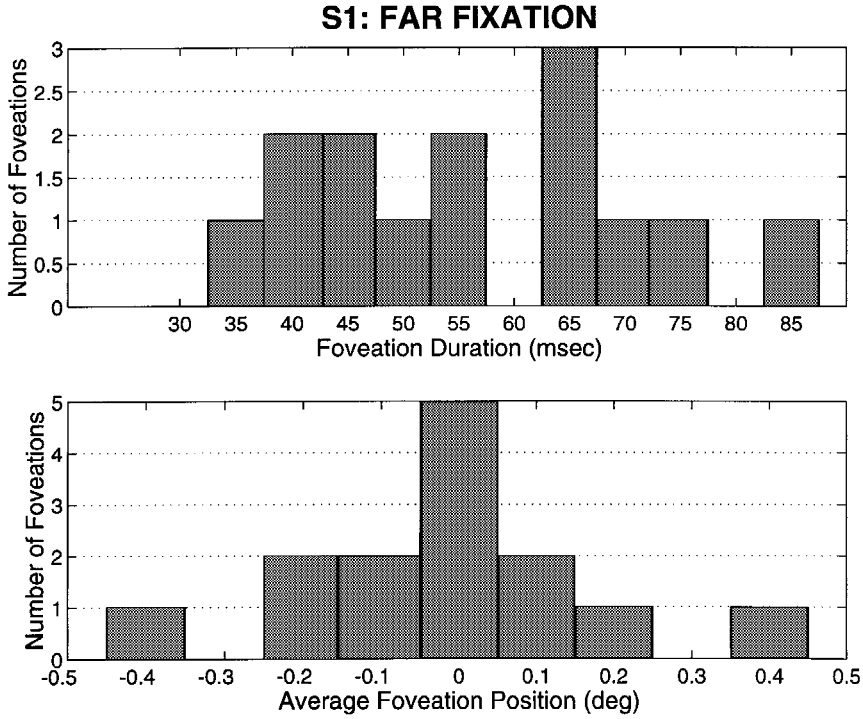

Figure 2b. (B) Example of output histograms for foveation-period duration (top) and average position (bottom). In Figures 2A, 4 and 7, the foveation windows are shown dashed.

of histograms. For this interval, most foveation periods averaged 40 – 65 ms in length and their average position was within $\pm 0.2°$ of the target.

Calculation of a representative τ-surface

Using the results of the above NAFX algorithm, a representative τ-surface for that data set was calculated by an adaptive, iterative algorithm that forced all NAFX values, calculated with all combinations of position and velocity boundaries for the foveation window, to be equal to the NAF for that data set. Figure 3 (top) shows the resulting representative τ-surface from which the appropriate value of τ is determined by the values of position and velocity chosen for the expanded foveation window.

Calculation of an average τ-surface

Representative τ-surfaces were calculated for five different data sets from S1, containing several CN waveforms. Finally, an average τ-surface was calculated and is shown in Figure 3 (middle) along with the skeletons of the

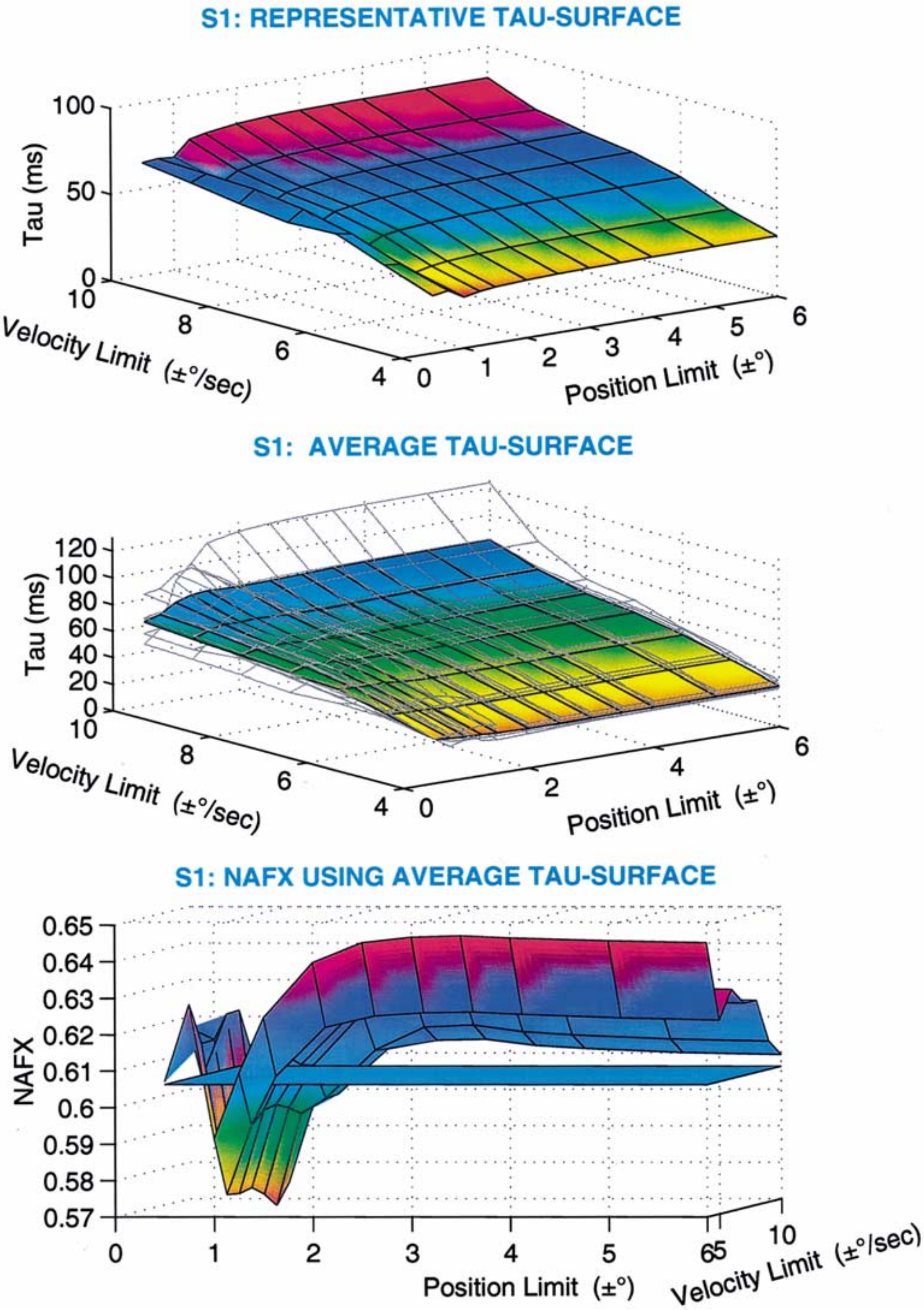
S1: REPRESENTATIVE TAU-SURFACE
Tau (ms)
100
50
0
10
8
6
4
Velocity Limit (±°/sec)
0
1
2
3
4
5
6
Position Limit (±°)
S1: AVERAGE TAU-SURFACE
Tau (ms)
120
100
80
60
40
20
0
10
8
6
4
Velocity Limit (±°/sec)
0
2
4
6
Position Limit (±°)
S1: NAFX USING AVERAGE TAU-SURFACE
NAFX
0.65
0.64
0.63
0.62
0.61
0.6
0.59
0.58
0.57
0
1
2
3
4
5
6
Position Limit (±°)
5
10
Velocity Limit (±°/sec)

five τ-surfaces that generated it. The average τ-surface was chosen for use in evaluating the NAFX for all further data sets.

Evaluation of the error-surface

As a final test of the accuracy of NAFX values calculated using the above average τ-surface (from S1) to calculate the NAFX values for each data set, individual error-surfaces were calculated. Figure 3 (bottom) also shows one such error-surface for one data set from S1. As can be seen by comparing the values of NAFX with the NAF value for that data set (0.61), the NAFX values are well within the design criterion of a $\pm 10\%$ error. The error surfaces for each of the other data sets also satisfied this design criterion.

Application of the NAFX to other subjects

The NAFX, derived as described above, was then used to determine the best-corrected visual acuity of other subjects, both with and without well-developed foveation. The expanded nystagmus acuity function is defined by:

$$NAFX = (1 - \sigma_{pv})[1 - \epsilon^{-t_f/\tau}]$$

where the pooled estimator

$$\sigma_{pv} = \sqrt{(SD_p^2 + SD_v'^2)/2}, \quad SD_v' = (p/v)(SD_v)$$

and t_f is the foveation-period duration. The foveation window may be any combination of position (p) and velocity (v) values between $\pm 0.5°$–$\pm 6°$ and $\pm 4°$/s–$\pm 10°$/s, respectively, and the time constant, τ is calculated from the average τ-surface. The default values of the foveation window are $\pm 0.5°$ and $\pm 4°$/s, giving a τ=33.3 ms and resulting in an NAFX that is exactly equivalent to the original NAF.

Subject 2 had achiasma, CN, strabismus, amblyopia and see-saw nystagmus. Her horizontal CN was a typical example of someone who does not have well-developed foveation during distance vision. Figure 4 (left) shows significant position jitter during this 5-s data set containing 19 expanded foveation periods (i.e., $\pm 2°$ by $\pm 4°$/s) on both pseudopendular with foveating saccades and pendular with foveating saccades waveforms. The error-surface

Figure 3. The representative τ-surface for the data set in Figure 2, the average τ-surface generated from 5 representative τ-surfaces from S1 (the latter are shown as skeletons), and an example of the error-surface generated from one data set from S1. The NAF value for that data set (at 0.61) is shown as the plane intersecting the error-surface.

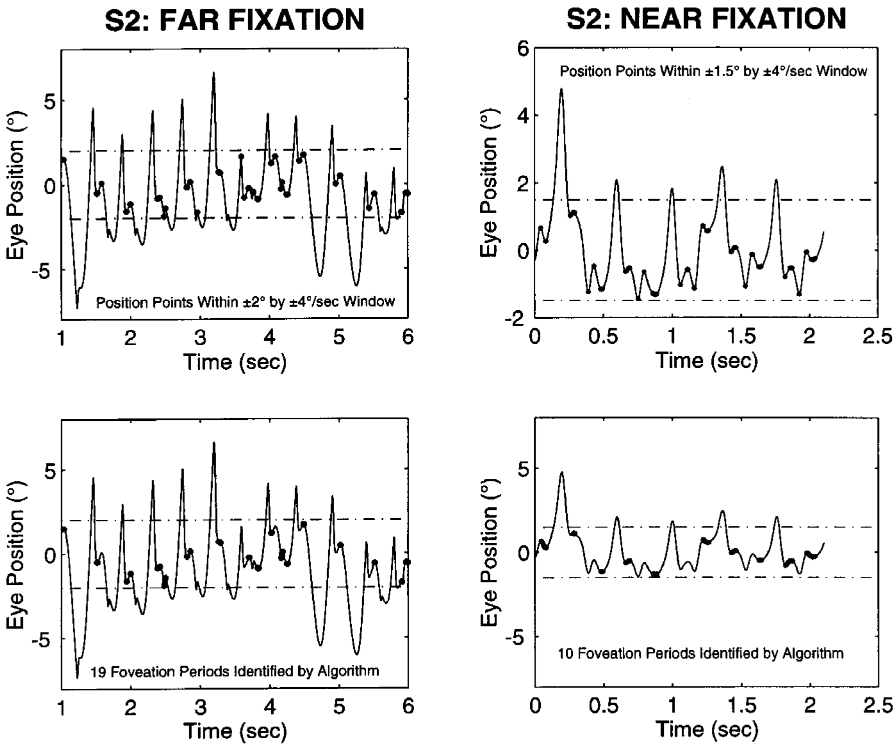

Figure 4. The NAFX 'showpv' algorithm's outputs for a 5-s interval of S2's far fixation and slightly over 2-s interval of S2's near fixation, showing both the data points (top) and foveation periods (bottom) satisfying the respective foveation-window criteria used (±2° by ±4°/s for far and ±1.5° by ±4°/sec for near). Nineteen foveation periods were identified for far (shown thickened) and 10 foveation periods for near. In Figures 4 and 7, the scales of the lower right plots were made equal to those on the lower left for ease of comparison of the resulting CN and NAFX windows.

for all NAFX values, calculated using the average τ-surface from S1, is well within ±1 Snellen line, as Figure 5 demonstrates. However, as Figure 4 (right) shows, this subject's foveation was better at near. The NAFX foveation window (±1.5° by ±4°/s) yielded 10 foveation periods (in this 2.1-s data set) within the pseudopendular with foveating saccades waveform.

Using the NAFX to assess the effects of vergence and gaze angle

To demonstrate the use of the NAFX to determine the conditions under which maximum acuity might be achieved, we also plotted S1's NAFX at different convergence angles (fixating targets at different distances) and S2's NAFX at different gaze angles for her preferred right-eye fixation and at near. Figure 6 (top) shows that there is a gradual increase in the NAFX as convergence angle

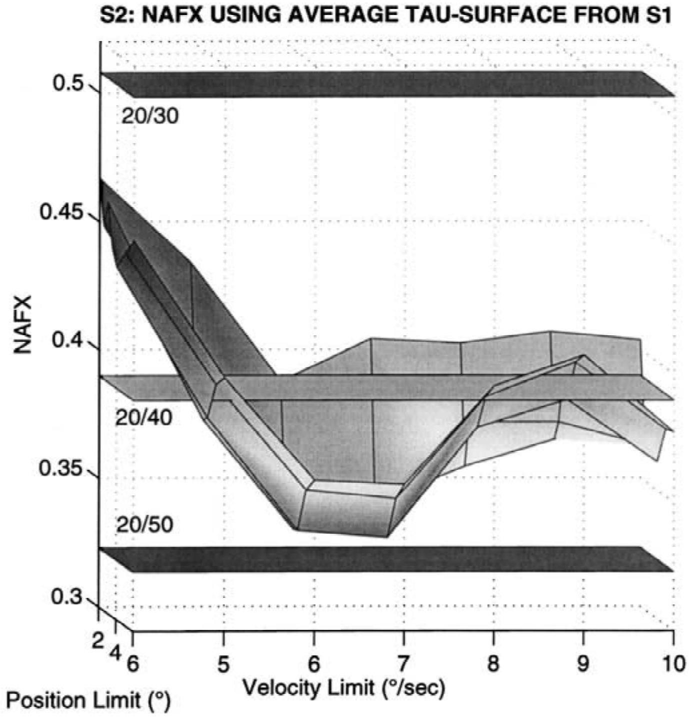

Figure 5. Example of the error-surface generated from the data in Figure 4. The NAFX values and equivalent best-corrected visual acuities are shown as planes.

increases from 2° (distant target) to a peak at 19.6° (target at 16.5 cm) and then a more rapid decrease as convergence further increases (target brought to 8.3 cm). We regard the sharp changes at 9 and 13° to reflect 'noise' in the data. To identify the range of gaze or convergence angles within which the subject's potential visual acuity is within 1 Snellen line of maximum, we define the *longest foveation domain* as the range between the points to either side of the peak NAFX that are 0.1 lower than that peak value. Thus, this domain in Figure 6 (top) is 20° (from 13° to 33° of convergence). Figure 6 (bottom) shows that S2 did not have a sharp peak of maximal NAFX (more predictive of highest acuity than a CN null) and that the two NAFX values (shown as shaded squares) measured at near from different data intervals were greater.

Using the NAFX to assess the effects of tenotomy

The first application of the new tenotomy procedure to damp CN was on an achiasmatic Belgian sheepdog [20]. Dogs have a 6° (horizontal) by 3° (ver-

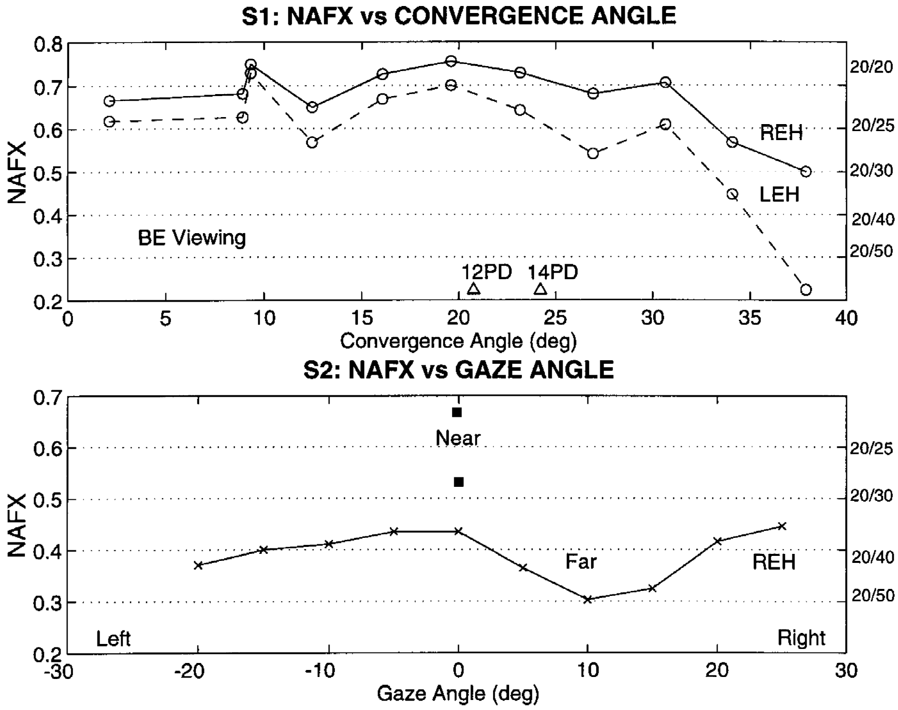

Figure 6. A plot of S1's NAFX values during fixation of near targets vs. the resulting convergence angle (top) and S2's NAFX values during fixation with the right eye at gaze angles ranging from –20° to +25° and at near (bottom). The absence of a large peak NAFX value indicates that there was no CN 'null' corresponding to an area of highest acuity. REH and LEH – right and left eye horizontal, respectively; triangles indicate equivalent convergence in prism diopters.

tical) *area centralis* instead of a fovea. As the pre-tenotomy data of Figure 7 show, the NAFX algorithms, using a ±3° by ±4°/s *centralisation* window, yielded 14 short foveation periods for this 4-second interval of pendular CN. Post-tenotomy, the same window yielded 16, much longer, foveation periods on a significantly damped pendular CN (also, Figure 7).

The NAFX vs. visual acuity (human and canine)

The NAF and NAFX values for nine subjects who had no afferent deficits and whose CN did not appear to change when viewing a Snellen chart are plotted against their measured acuity in Figure 8. The mean NAF (and the SD) values were calculated from twenty, 2-s intervals in a 20-s record for each subject. Each 2-s interval overlapped its contiguous 2-s intervals by 1 second [9]. Unlike the procedure outlined in the 'Methods', no attempt was

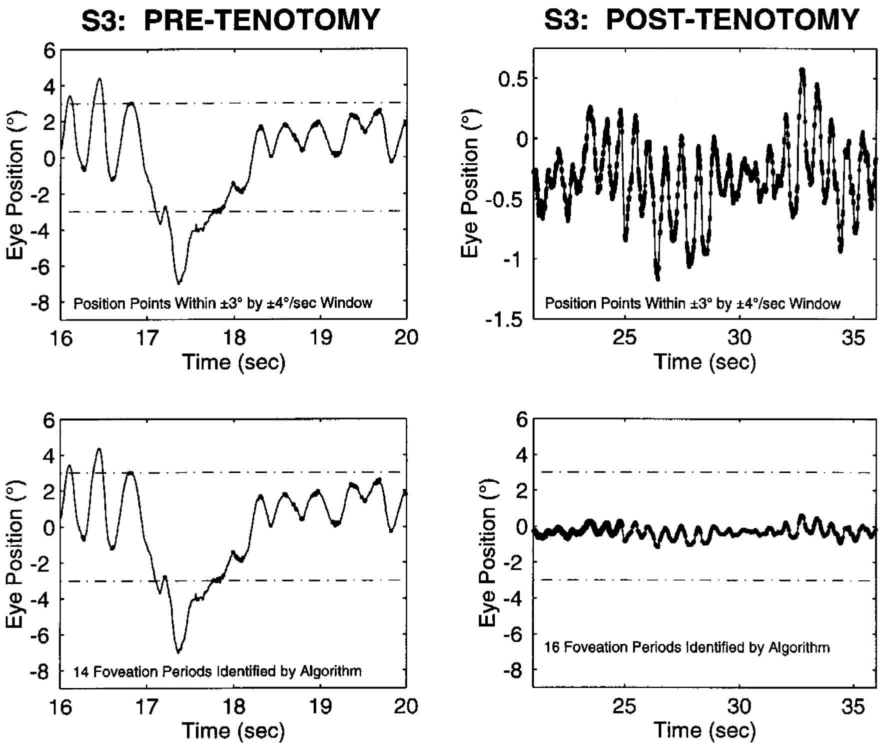

Figure 7. The NAFX 'showpv' algorithm's outputs for a 4-s interval of S3's pre-tenotomy far fixation and a 15-s interval of S3's post-tenotomy far fixation, showing both the data points (top) and foveation periods (bottom) satisfying the default canine centralisation-window criteria (equal to an expanded foveation-window criteria of ±3° by ±4°/s). Fourteen centralisation periods were identified pre-tenotomy (shown thickened) and 16, *very long*, centralisation periods were identified post-tenotomy.

made to eliminate blinks or other intrusions on fixation. In contrast, the individual NAFX calculations (3 shown for each subject) were made using the different foveation-window sizes that resulted from applying the procedure outlined in the Methods. Position sizes ranged from 0.5 to 2.5° and velocity sizes ranged from 4 to 9°/s. Typical measured values of NAF and NAFX for S1 and S2 are plotted in Figure 9 vs. their *measured* best-corrected visual acuities. For S2, her better (right) eye was used (OD: 20/60, OS: 20/100, OU: 20/50 with the right eye fixating). Also plotted for comparison is the NAF vs. *predicted* best-corrected visual acuity line. For the canine subject (S3), we plotted three pre- and one post-operative NAFX values vs. visual acuity and based our NAF vs. best-corrected visual acuity line (dashed) on a canine acuity limit of approximately 20/75 [21,22]. That is, the NAFX vs. canine acuity line is a presumption based on canine acuity data and the data points

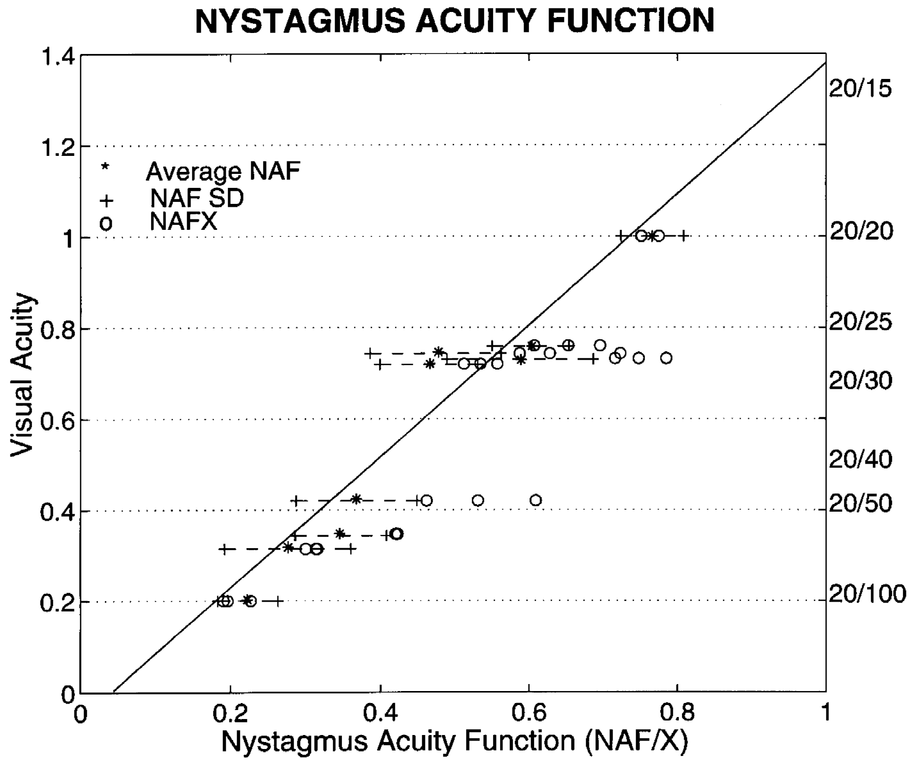

Figure 8. Data from nine CN subjects with neither afferent deficits nor significant fixation-attempt effects on their waveforms, showing the linear relationship between the NAF and potential, best-corrected visual acuity and the equivalent NAFX values calculated using arbitrary foveation-window sizes, determined as explained in the Methods. For clarity, the data points for two individuals (mean NAF's of 0.588 and 0.602) were slightly lowered or raised respectively. Each individual had the same acuity (0.743 = 20/25-3) as the individual whose data are straddled (mean NAF of 0.478).

do not reflect actual acuity measurements, but presumed improvement based on immediate and lasting changes in behavior. The important information is that the increase in the NAFX value after tenotomy ranged from 37% to 77% over the pre-tenotomy values – the surgery was a success.

Discussion

Visual acuity and congenital nystagmus

Visual acuity is dependent on the optical media, afferent neurophysiology and ocular motor stability. Optically, refractive errors or corneal, lens, or vitreous

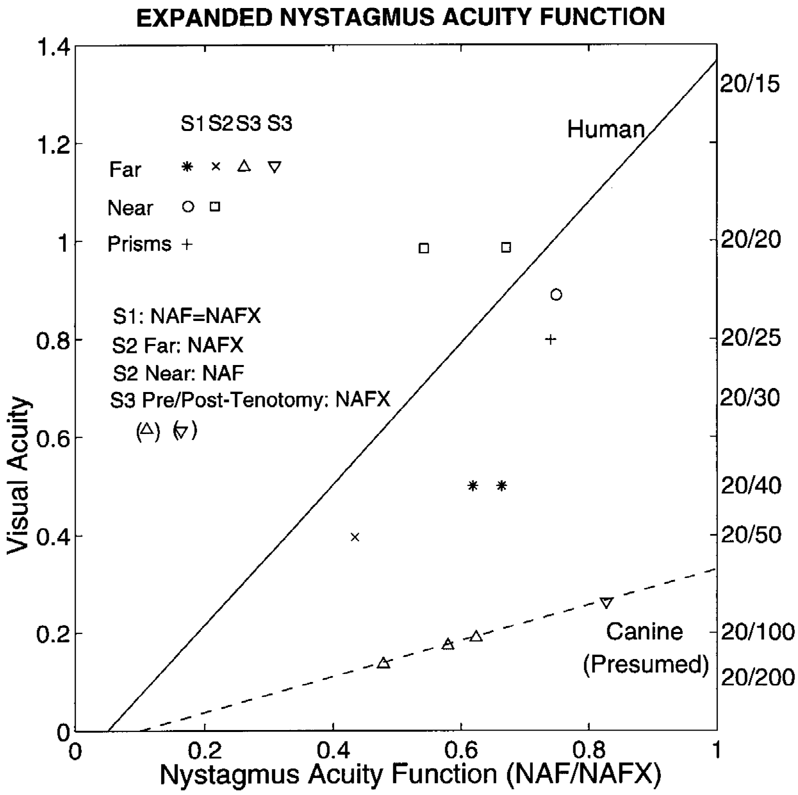

Figure 9. The NAFX values of S1 and S2 plotted vs. measured visual acuity at far and near along with the NAFX vs. best-corrected possible visual acuity line (solid) and the pre- and post-tenotomy NAFX values of S3 plotted vs. the *presumed* canine best-corrected possible visual acuity line (dashed). For S1 the two points for distance fixation are average values for the left- (lower) and right- (higher) eye fixation; the NAF value for far fixation using composite (i.e. unequal) converging prisms is also shown. For S3, three pre-tenotomy NAFX values are shown along with the higher post-tenotomy value, arbitrarily plotted on the canine acuity line.

abnormalities can reduce acuity. Afferent defects in the retina, fovea, optic nerves, etc. can also reduce acuity. Finally, ocular motor instability, due to nystagmus or saccadic oscillations, can reduce acuity. If the nystagmus is CN, the additional input of psychological stress (e.g. anxiety, anger, fear, etc.) will increase the CN and further reduce acuity [23]. These factors interact in a nonlinear manner, making the prediction of actual visual acuity, based on only one of them a problematic undertaking. The use of the NAF to predict best-corrected visual acuity possible, based on the effects of retinal image motion due to CN (or other nystagmus), is subject to these problems. To reduce the other effects as much as possible, the NAFX is calculated from data taken during non-stressful viewing of an LED, using intervals characteristic of the subject's CN under these relaxed conditions. That is, intervals with transient changes in the waveform (either detrimental or beneficial to vision) are excluded from consideration (e.g. blinks, saccades off target, longer than usual foveation periods, etc.); only intervals containing the repeatable waveform of the subject are used. In addition, the generation of an average τ-surface was accomplished by forcing the NAFX to equal the NAF for all values of position and velocity boundaries since the subject's visual acuity does not change just because we choose a different foveation window within which to calculate the NAFX.

As Figure 8 demonstrates, the resultant NAFX is linearly related to potential, best-corrected visual acuity based on the nystagmus alone and extends the NAF's ability to predict potential acuity. Because the data for Figure 8 came from subjects who exhibited well-developed foveation (allowing the use of the original NAF), had no afferent deficits, and whose CN did not appear to change during acuity testing, they were expected to be able to utilize 100% of the potential acuities predicted by the NAF. Their data points were used to generate the NAF vs. acuity line [9]. The lower mean NAF values of some subjects when compared to their more recently calculated NAFX values and the higher SD's for each subject reflect the arbitrary method of choosing each 2-s interval for analysis of the original NAF. However, using only intervals without interruptions to fixation, as described in the Methods for the NAFX, resulted in slightly higher values and lower SD's for some subjects. The NAFX values yield a more accurate prediction of potential visual acuity for each subject. Some of these subjects had consistent waveforms and foveation whereas others showed variation in both over the 20-s data intervals; that accounted for the differences in SD's. For those subjects whose NAFX values were higher than the original NAF values, either their data contained significant intervals of poor foveation or their waveforms did not remain constant during acuity testing. If, at the other end of the subject spectrum, NAFX's were calculated for subjects with CN and *no light perception*, the data points would all fall *on the x-axis*. Such individuals would not be able to utilize *any* of the potential acuity predicted by the NAFX analysis of their CN waveforms. For most individuals with CN, the presence of any of the non-waveform factors that might decrease acuity directly or adversely affect the CN waveform will lower the measured Snellen acuity below the NAFX-predicted value in a nonlinear and idiosyncratic manner and their data points will fall between the NAFX vs. acuity line and the x-axis [9].

Calculation and use of the NAF(X)

The current algorithm for calculating the NAFX does so automatically and with minimal human intervention. It represents a large step forward from the original NAF in both its applicability to most, if not all, CN subjects (including non-human subjects) and in the reduction of the expertise necessary to use it accurately. Because additional, short foveation intervals may be included in bidirectional CN waveforms, the current algorithm may yield slightly lower NAFX values in certain limited cases as the foveation window is enlarged from its default to approximately $\pm 3°$. We are currently working on the next-generation algorithm that should alleviate this tendency. However, by following the steps outlined in the 'Methods' section, the current NAFX has been applied to many subjects whose CN waveforms and foveation ability has covered a broad spectrum. Through the use of this standardized protocol, the resulting values were unbiased predictions of the best-corrected visual acuity possible with that particular waveform. By constraining the calculation of the average τ-surface to be within $\pm 10\%$, we tried to ensure that, when applied to a subject without well-developed foveation, the acuity predicted by the NAFX would remain within one Snellen line, regardless of the dimensions of the foveation window used in its calculation (see Figures 5 and 8). In Figure 8, the predicted acuities of the NAFX points shown are within ± 1 Snellen line of their mean values.

For individual subjects, the NAFX clearly demonstrates differences in possible acuity due to convergence (compare Figures 4, 6 and 9) or gaze angle (Figure 6). For S1, the NAFX demonstrated that there was an *optimal* convergence angle, beyond which the NAFX and expected acuity declined and that range within which visual acuity could be expected to be within one Snellen line of the peak acuity is given by the longest foveation domain value of 20°. Also shown in Figure 6 (top), are the convergence angles produced by 6 and 7 PD BO prisms (12 and 14 total PD, respectively). S1 had been wearing 7 PD BO for many years with excellent results but the NAFX suggests that a relaxation to 6 PD BO would provide as good or better acuity; both values are within the longest foveation domain. The NAFX for S2 during right-eye fixation does indicate better acuity from primary position to slight left gaze. This is consistent with S2's preference for using her right eye to fixate in left gaze; S2 did not have a pronounced head-turn. Due to her strabismus, the higher NAFX at near could not be therapeutically exploited by *either* base-out prisms or bimedial recession surgery. The data intervals we chose to illustrate S1's distance acuity in Figure 9 were typical, with NAF's ($*$) that predicted a slightly higher potential acuity (20/25) than the 20/40 actually measured. The difference between the measured and best-possible acuity reflects the intensification of the CN waveforms during acuity testing compared to the better waveforms resulting from the relaxed conditions used to calculate the NAF. Under stress, S1's acuity dropped below 20/40. However, at near and with composite base-out prisms (OD: 11 PD, OS: 3 PD), the CN was sufficiently damped even during acuity measurement to yield both higher NAF and measured acuity values. The NAFX values at near for S2 also reflect the improvement in acuity from that at far and predict a visual acuity between 20/30 and 20/20; the measured acuity at near was 20/20. The slightly higher acuity may be due to: differences in near vs. far acuity; using data taken at a convergence angle beyond that resulting in the highest NAFX; or the fact that the NAFX was derived to predict far acuity. Some of the difference may also be related to the effect on the NAFX algorithm of extra foveation intervals detected as the CN damps at near (see Figure 4). Finally, for subjects with CN, the NAFX provides an objective measure of the effects on CN waveform of therapeutic intervention (e.g. prisms for S1 and tenotomy for S3) on predicted best-corrected acuity (see Figures 6, 7 and 9).

The NAF(X)

The original NAF was developed from normal anatomical and physiological data plus the effects of foveation duration, beat-to-beat accuracy and velocity variation [9]. It is an objective measure of the foveation ability of CN waveforms and, therefore, of potential visual acuity that could be used to evaluate the effects of therapies applied to a patient or across patients. The measure also had to be useful for intersubject comparisons if different therapies were to be compared. A major problem with measuring visual acuity at the Snellen chart is the variable extent that stress alters the CN and, therefore, the acuities of different patients. After a procedure, it is not unusual for a patient to see better, and so inform the physician, but to fail to demonstrate significant improvement at the Snellen chart. Similarly, it is common for some patients' Snellen acuities to exceed that required for a driving license when measured in the ophthalmologist's office but not at the time of testing at the Motor Vehicle Bureau. The problem is the deleterious effect of stress on the CN and the resulting reduction in acuity.

By design, the NAF circumvented this problem and objectively measured the direct effects of a therapy on improving the quality of the CN waveform; that is what CN therapies are designed to do. If the CN waveform was changed in a manner conducive to improved acuity (e.g. longer foveation times, less jitter, etc.), the NAF increased and the therapy was considered a success despite the possibility that the measured Snellen acuity may not have improved due to factors unrelated to the CN. Indeed, for those with severe limitation of their acuity imposed by afferent deficits, no measurable acuity improvement *should* be expected as a result of a therapy aimed at damping the CN alone, although improvement may result in some individuals. The NAFX extends this objective measure of the effects on the CN waveform and its relationship to best-possible acuity to most, if not all, individuals with

CN and other types of nystagmus. Over the past 8 years for the NAF and 3 years for the NAFX, this software has undergone extensive development and refinement in the Ocular Motor Neurophysiology Lab and has been applied to subjects with a wide variety of CN and LMLN waveforms. The application methodology (see 'Methods') also reflects several years of refinement and standardization, based on the analysis of subjects with a wide variety of nystagmus waveforms who were studied in our laboratory. The resulting NAFX is a reliable, acuity-sensitive function that is currently being used as the *primary measure* in two clinical studies of the effects of the tenotomy procedure as a treatment of human CN. The NAFX-derived longest foveation domain is also being used to determine the amount of broadening of the range of gaze angles of highest acuity produced by tenotomy. This measure is similar to the null-broadening hypothesized to be due to tenotomy but is more directly related to potential visual acuity than measurement of the null region based simply on CN amplitude.

Acknowledgements

This work was supported in part by the Office of Research and Development, Medical Research Service, Department of Veterans Affairs.

Appendix

Command lines and outputs of the NAFX program

---

* ≪ nff1(lh,lhv,488,[0.5,5],'showpv',1); [MATLAB command line]
* Total time that meets position criterion = 2725.4098 ms. (1330 samples)
* Total time that meets velocity criterion = 1508.1967 ms. (736 samples)
* Total time that meets both criteria = 1202.8689 ms. (587 samples)
* There were (probably) 19 foveation periods in this interval.
* Display foveation statistics (y/n)? y [MATLAB prompt line]

* Foveation #1: duration 102.459 ms, Avg pos –1.9403 deg
* Foveation #2: duration 43.0328 ms, Avg pos 0.98586 deg
* Foveation #3: duration 131.1475 ms, Avg pos 0.43795 deg
* Foveation #4: duration 8.1967 ms, Avg pos –3.5244 deg
* Foveation #5: duration 45.082 ms, Avg pos 0.058937 deg
* Foveation #6: duration 57.377 ms, Avg pos 0.70115 deg
* Foveation #7: duration 116.8033 ms, Avg pos –0.74789 deg
* Foveation #8: duration 28.6885 ms, Avg pos 0.09037 deg
* Foveation #9: duration 61.4754 ms, Avg pos –0.43728 deg
* Foveation #10: duration 12.2951 ms, Avg pos –3.6794 deg
* Foveation #11: duration 59.4262 ms, Avg pos –0.045185 deg
* Foveation #12: duration 8.1967 ms, Avg pos 3.5244 deg
* Foveation #13: duration 51.2295 ms, Avg pos 0.20855 deg
* Foveation #14: duration 90.1639 ms, Avg pos –1.4459 deg
* Foveation #15: duration 55.3279 ms, Avg pos –0.3873 deg
* Foveation #16: duration 63.5246 ms, Avg pos –0.59306 deg
* Foveation #17: duration 18.4426 ms, Avg pos –3.7956 deg
* Foveation #18: duration 10.2459 ms, Avg pos –2.937 deg
* Foveation #19: duration 14.3443 ms, Avg pos –1.3556 deg

* ≫nff1(lh,lhv,488,16,'nafx',[0,0.5,5]); [MATLAB command line]
* NAFX results:
* NAF(X) = 0.64911 deg <–[<=]–> 20/25+- [Equivalent Snellen acuity]
* NAF(X) (for position only) = 0.68047
* Foveation time per fov period = 75.1793 ms
* Foveation time per second = 0.24057 s
* STD(pos) = 0.18105 deg
* STD(vel) = 2.5092 deg/s
* Foveation window (position): 0.5 deg
* Foveation window (velocity): 5 deg/s
* tau: 42.3 ms

In both command lines, 'lh' and 'lhv' are arrays that determine the position and velocity intervals, 488 is the sampling frequency of the digitized data, '[0.5,5]' specifies the expanded foveation window used, the '1' in the 'showpv' command line toggles between two displays (0/1), the '16' in the 'nafx' command line indicates the number of cycles in the interval (determined from the 'showpv' display), and the '0' of '[0,0.5,5]' sets τ to the value specified by the default τ-surface. The equivalent Snellen output indicates the maximum acuity predicted by the NAFX value. As shown above, the software can also display duration and average position data about each foveation period, when prompted to do so.

References

1. Dell'Osso LF, Gauthier G, Liberman G, Stark L. Eye movement recordings as a diagnostic tool in a case of congenital nystagmus. Am J Optom Arch Am Acad Optom 1972; 49: 3–13.
2. Dell'Osso LF. Fixation characteristics in hereditary congenital nystagmus. Am J Optom Arch Am Acad Optom 1973; 50: 85–90.
3. Dell'Osso LF, Flynn JT, Daroff RB. Hereditary congenital nystagmus: An intrafamilial study. Arch Ophthalmol 1974; 92: 366–374.
4. Dell'Osso LF, Flynn JT. Congenital nystagmus surgery: a quantitative evaluation of the effects. Arch Ophthalmol 1979; 97: 462–469.
5. Bedell HE, Loshin DS. Interrelations between measures of visual acuity and parameters of eye movement in congenital nystagmus. Invest Ophthalmol Vis Sci 1991; 32: 416–421.
6. Dickinson CM, Abadi RV. The influence of nystagmoid oscillation on contrast sensitivity in normal observers. Vision Res 1985; 25: 1089–1096.
7. Abadi RV, Worfolk R. Retinal slip velocities in congenital nystagmus. Vision Res 1989; 29: 195–205.
8. Dell'Osso LF, Van der Steen J, Steinman RM, Collewijn H. Foveation dynamics in congenital nystagmus I: Fixation. Doc Ophthalmol 1992; 79: 1–23.
9. Sheth NV, Dell'Osso LF, Leigh RJ, Van Doren CL, Peckham HP. The effects of afferent stimulation on congenital nystagmus foveation periods. Vision Res 1995; 35: 2371–2382.
10. Abadi RV, Dickinson CM. Waveform characteristics in congenital nystagmus. Doc Ophthalmol 1986; 64: 153–167.
11. Ukwade MT, Bedell HE. Variation of congenital nystagmus with viewing distance. Optom Vis Sci 1992; 69: 976–985.
12. Currie DC, Bedell HE, Song S. Visual acuity for optotypes with image motions simulating congenital nystagmus. Clin Vis Sci 1993; 8: 73–84.
13. Graham CH, Cook C. Visual acuity as a function of intensity and exposure-time. Am J Psychol 1937; 49: 654–661.
14. Keesey UT. Effects of involuntary eye movements on visual acuity. J Opt Soc Am 1960; 50: 769–774.
15. Abadi RV, Dickinson CM, Pascal E, Whittle J, Worfolk R. Sensory and motor aspects of congenital nystagmus. In: Schmid, R, Zambarbieri, D, eds. Ocular Motor Control and Cognitive Processes. Proceedings of the 5th European Conference on Eye Movements. North Holland, Elsevier Science Publishers BV, 1991: 249–262.
16. Dell'Osso LF, Leigh RJ, Sheth NV, Daroff RB. Two types of foveation strategy in 'latent' nystagmus. Fixation, visual acuity and stability. Neuro Ophthalmol 1995; 15: 167–186.
17. Jacobs JB, Dell'Osso LF. An expanded nystagmus acuity function [ARVO Abstract]. Invest Ophthalmol Vis Sci 1998; 39: S149.
18. Leigh RJ, Rushton DN, Thurston SE, Hertle RW, Yaniglos SS. Effects of retinal image stabilization in acquired nystagmus due to neurological disease. Neurology 1988; 38: 122–127.
19. Steinman RM, Collewijn H. Binocular retinal image motion during active head rotation. Vision Res 1980; 20: 415–429.
20. Dell'Osso LF, Hertle RW, Williams RW, Jacobs JB. A new surgery for congenital nystagmus: Effects of tenotomy on an achiasmatic canine and the role of extraocular proprioception. J Am Assoc Pediatr Ophthalmol Strab 1999; 3: 166–182.

21. Miller PE, Murphy CJ. Vision in dogs. J Am Vet Med Assoc 1995; 207: 1623–1634.
22. Budiansky S. How do the hunted view the hunter? The Field 1999(September): 42–45.
23. Dell'Osso LF. Improving Visual Acuity in Congenital Nystagmus. In: Smith JL, Glaser, JS, eds. Neuro-Ophthalmology Symposium of the University of Miami and the Bascom Palmer Eye Institute, vol. VII. St. Louis, CV Mosby Company, 1973: 98–106.

Address for correspondence: L.F.Dell'Osso, Ocular Motor Neurophysiology Laboratory, Veterans Affairs Medical Center (127A), 10701 East Boulevard,
Cleveland, OH 44106, USA
Phone: 216-421-3224; Fax: 216-231-3461; E-mail: ifd@po.cwru.edu